Network defects and molecular mobility in liquid water

Francesco Sciortino
Center for Polymer Studies and Department of Physics, Boston University, Boston, Massachusetts 02215

Alfons Geiger
Physikalische Chemie, Fachbereich Chemie der Universität Dortmund, Postfach 500500, D-4600 Dortmund 50, Germany

H. Eugene Stanley
Center for Polymer Studies and Department of Physics, Boston University, Boston, Massachusetts 02215

As a step toward elucidating the connection between the structure and mobility of liquid water, we analyze quenched molecular dynamics configurations at different densities. We find that the mobility is directly related to the existence of "topological defects" of the tetrahedral network. The defects act as catalysts, providing lower energy pathways between different tetrahedral local arrangements.

INTRODUCTION

Two decades of computer simulation studies on water and aqueous solutions have immensely broadened our knowledge about this ubiquitous and unusual liquid.[1-7] It is now possible to reproduce in a molecular dynamics (MD) simulation a wide range of measurable properties of water, from thermodynamics to structure and microdynamics. Thus one is encouraged to use the simulations to examine features that are not directly measurable, but of central importance for the understanding of water structure and dynamics.

From such computer simulations, it is well known that liquid water is a totally connected random network of hydrogen bonds (HB)—well above the percolation threshold.[8,9] The strength of a typical HB in water is roughly 20 kJ/mol, a value much larger than kT. Hence one should expect water to behave like a stable network. In contrast to this expectation, the HB network restructures itself on a picosecond time scale.[1-10] The water molecules are found to display a high mobility, comparable to molecules in nonhydrogen bonded liquids.

Many experiments indicate that the random tetrahedral network *cannot be perfect*, but must contain some sort of structural defect associated with a local region of higher density.[11] Indeed, the integral over the first peak of the oxygen distribution function from x-ray scattering shows that there are on average more than four water molecules ("extra molecules") in the first coordination shell; specifically, the coordination number is about 4.5 (Ref. 12). Moreover, Raman data have been interpreted in terms of local structural defects associated with a different kind of bonding: instead of a proton engaging in one hydrogen bond (a "linear bond"), it engages in two (a "bifurcated bond").[13] At ambient temperature these bifurcated bonds appear to make a significant contribution to the Raman spectrum.[14]

The importance of such network defects for the mobility of the water molecules has been supported by experiments[15] and simulations.[16] In contrast to the behavior of normal liquids (described by the free volume theory[17]), a density decrease in water leads to a slowing down of the rotational and translational single particle diffusion. The simulations in the stretched region (density less than equilibrium) show that the decrease in molecular mobility on lowering the density correlates with the decrease in (i) the number of water molecules found within the first coordination shell, and (ii) the fraction of water molecules with more than four intact HBs. Both (i) and (ii) indicate the presence of defects in the perfect four-coordinated network whose number decreases on lowering the density, and suggests that the decrease in mobility at low density is directly associated with a decrease in the number of defects.

These local network defects contained in the tetrahedral water network have recently been investigated by MD simulation. The HB interactions were classified in groups according to the number of bonds in which each proton is involved.[18] Although each group is characterized by a broad distribution of angles and energies, the sum of the characteristic energy of the two bonds in the bifurcated arrangement were found to be roughly the same as the characteristic energy of a linear bond. This led to the suggestion that the bifurcated bonds may represent local arrangements which facilitate the switching from one "regular" HB arrangement to another across lowered energy barriers.[18,19]

In this paper we examine the effect of defects in the tetrahedral network of water on molecular mobility. We analyze quenched configurations, representing the "inherent" structure of the liquid.[20] Since only local minima survive the quench process, the quenched state represents the structure of the liquid without "vibrational" distortions. The analysis of the bonding as well as of the structure is less ambiguous if performed after subtracting such thermal vibrations[21] since a clear distinction between purely thermal displacements and real or inherent defects can be made.

We shall argue that such "topological defects" affect the mobility by providing lower energy pathways between different tetrahedral local arrangements. That is, the presence of a fifth molecule acts as "catalyst" for the restructuring of the HB network even though the thermal energy kT is much smaller than the HB energy. To study the role of these defects, we change their concentration and explore the effect of such a change on molecular mobility. We tune the defect

concentration not by changing the temperature but by changing the density of the simulated system,[16] thereby enabling us to separate contributions to the mobility arising from thermal effects from contributions related to the defect concentration. It is hoped that our results serve to motivate more experimental effort to study "stretched" water, as initiated recently by Angell.[22]

COMPUTATIONAL PROTOCOL

Our simulations concern a system of 216 water molecules interacting via the ST2 potential.[2] We perform simulations at constant density and constant energy (the NVE ensemble). The direct molecular interactions up to the cutoff distance $r_c = 7.8$ Å are combined with a reaction field approximation for more distant pairs. The density is decreased in steps from $\rho = 1.0$ to 0.75 g/cm³. Two parallel simulation series were performed, with average temperatures of 273 and 235 K. Before the actual simulations were started, equilibration runs (extending up to 300 ps at low temperatures or densities) were applied. For further description of the computational techniques, see Ref. 16. We choose to study the

"low" temperature of $T = 235$ K to facilitate the recognition of effects related to the temperature.

From each simulation we extract between 50 and 100 equally spaced configurations (corresponding to a time interval between configurations ranging from 0.2 to 0.6 ps). We then calculate the respective "quenched" (or inherent) configurations using a two-stage procedure[20]:

(i) A fast removing of the kinetic energy, by applying a strong damping to the equations of motion;

(ii) A steepest descent numerical calculation to move the molecules along the potential energy surface toward the local minimum. The steepest descent procedure is performed until the fractional change in potential energy between successive steps is less than 10^{-5} kJ/mol. (We tested our results by performing a calculation with 10^{-6} kJ/mol and found essentially the same results.)

STRUCTURE

We begin by examining the structural changes that occur in the quenched configurations when the density is changed at constant temperature. Figure 1(a) shows for
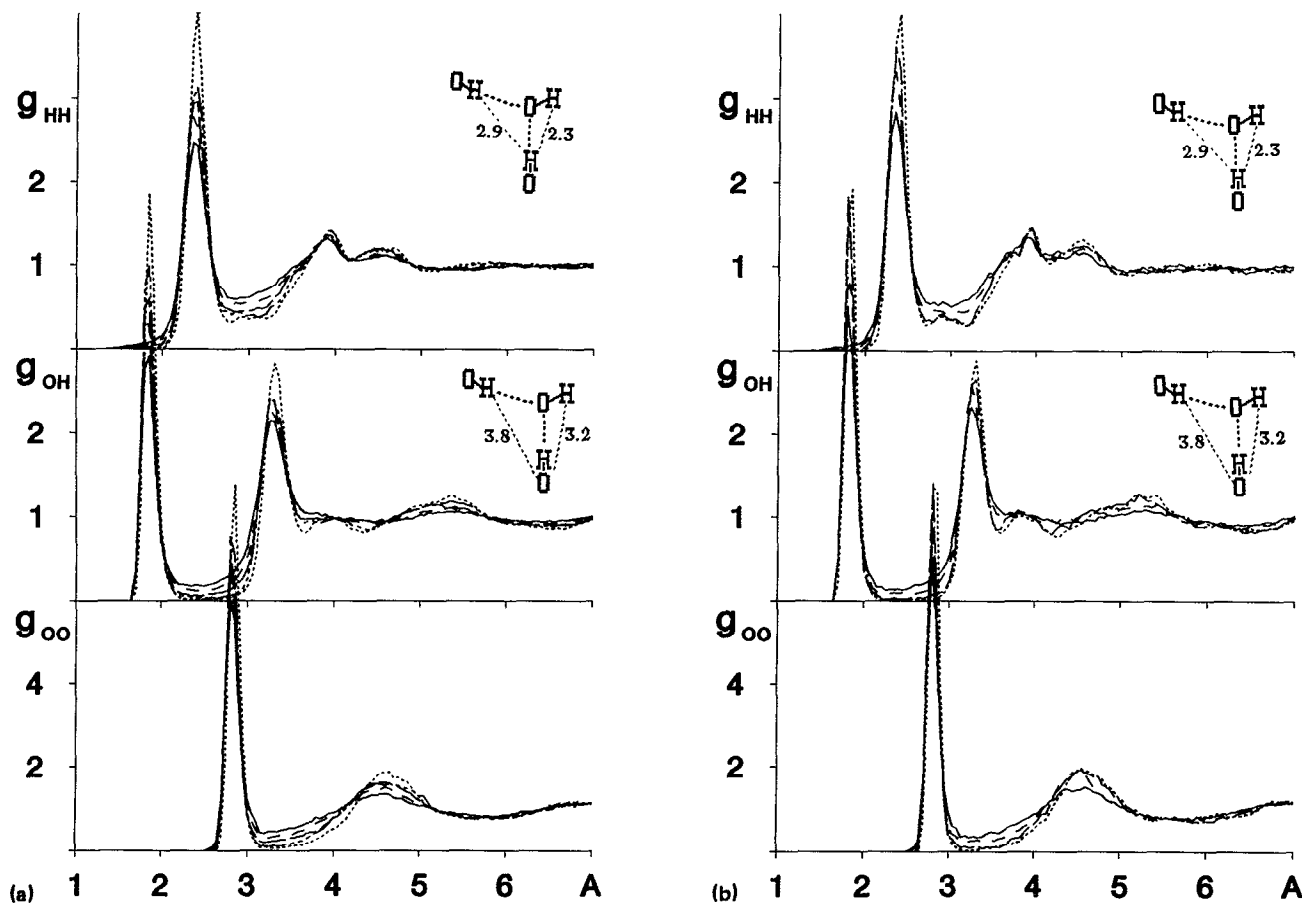

FIG. 1. (a) HH, OH, and OO radial distribution functions g_{HH}, g_{OH}, and g_{OO} for quenched configurations at temperature $T = 273$ K, as the density is decreased stepwise from $\rho = 1.0$ g/cm³: $\rho = 1$ (solid curve), 0.95 (small broken curve), 0.9 (large broken line), 0.85 (long and short dashes), and 0.8 (dotted). (b) HH, OH, and OO radial distribution functions for quenched configurations at temperature $T = 235$ K as the density is decreased: $\rho = 1$ (solid curve), 0.95 (small broken), 0.88 (large broken line), 0.83 (dotted). The insets show the first and second neighbor HH and OH distances calculated from the structure of ice.

TABLE I. The fraction of molecules with j neighbors within a distance $r = r_{min} = 3.3$ Å for $T = 273$ and $T = 235$ K, as calculated from the quenched configurations. Values for liquid and amorphous Si, obtained from Ref. 30, are shown for comparison.

				$T = 273$ K			
	$j = 2$	3	4	5	6	7	8
$\rho = 1.00$	0.0	3.6	46.2	33.6	12.7	3.0	0.9
$\rho = 0.95$	0.1	3.9	59.8	26.8	7.9	1.2	0.3
$\rho = 0.90$	0.2	5.0	75.6	16.5	2.3	0.3	0.0
$\rho = 0.85$	0.3	5.2	84.4	9.3	0.7	0.0	0.0
$\rho = 0.80$	0.4	7.9	87.8	3.6	0.1	0.0	0.0
$\rho = 0.75$	1.0	9.7	83.9	4.6	0.5	0.0	0.0
				$T = 235$ K			
	$j = 2$	3	4	5	6	7	8
$\rho = 1.00$	0.0	1.6	52.1	31.3	11.4	2.9	0.5
$\rho = 0.95$	0.0	1.3	71.3	19.7	6.1	1.1	0.2
$\rho = 0.88$	0.0	1.4	88.4	9.5	0.6	0.0	0.0
$\rho = 0.83$	0.4	3.0	92.3	3.8	0.4	0.0	0.0
				Values for Si			
	$j = 2$	3	4	5	6	7	8
Amorphous Si $T = 300$ K	0.0	0.6	78.0	21.0	0.3	0.0	0.0
Liquid Si $T = 1665$ K	0.0	2.0	29.0	48.0	19.0	2.0	0.0

$T = 273$ K the hydrogen–hydrogen (HH), oxygen–hydrogen (OH), and oxygen–oxygen (OO) radial distribution function $g_{HH}(r)$, $g_{OH}(r)$, and $g_{OO}(r)$ as the density is decreased from 1.0 to 0.80 g/cm^3. We observe an increase of the amplitude of the first and second neighbor peaks as well as a decrease of the first minimum, corresponding to progressive ordering of the liquid on lowering the density. The *ordering* of water on lowering the density is opposite to the behavior of simple liquids, for which lowering the density leads to a less pronounced, "smeared-out" structure, with smaller peaks in the radial distribution functions. We also note the presence of "isosbesticlike" points in the $g_{OO}(r)$ at 2.9, 4.2, and 5.2 Å, for $\rho \geqslant 0.85$. Recently, it has been argued that this effect is consistent with the possibility that water molecules can exist in distinct configurations characterized by four or more than four neighbors in the first coordination shell.[18]

On lowering the density below $\rho \approx 0.85$, secondary peaks emerge from the smeared out curves at higher densities—at approximately 4 Å in $g_{OH}(r)$ and at about 3 Å in the $g_{HH}(r)$. These peaks are associated with the proton ordering along the bonds up to the second neighbor, as shown in Fig. 1(a). Also at $\rho \approx 0.85$, we observe the disappearance of the isosbesticlike points in the $g_{OO}(r)$ and a very small shift in the position of the first and second peak corresponding to a slight stretching of the bond. As will be discussed below, these phenomena are related to the increase of three-coordinated molecules (i.e., to the actual breaking of a bond—i.e., the occurrence of "dangling" hydrogens), and may correspond to the network becoming close to its mechanical stability limit.[23]

The interpretation of the preceding paragraphs is supported by Fig. 1(b), which is the analog of Fig. 1(a) for $T = 235$ K. The peaks at approximately 4 Å in the $g_{OH}(r)$

and about 3 Å in the $g_{HH}(r)$ become more pronounced due to the further ordering produced by lowering the temperature.

We also studied the changes in the first coordination shell on lowering the density by calculating the average number of molecules $\langle n(r_{min}) \rangle$ within a sphere of radius $r_{min} = 3.3$ Å. Here r_{min} is the position of the first minimum in the $g_{OO}(r)$, as can be seen from Fig. 1. Only as $\rho \to 0.85$ g/cm^3 does $\langle n(r_{min}) \rangle \to 4$. Although a small temperature effect is observed, the dominant effect is associated with density change.

To characterize the distribution of neighbors, we show in Table I the number of molecules with j neighbors within the same distance r_{min}. The number of molecules with four neighbors increases at the expense of higher coordinated molecules, consistent with the interpretation that the main imperfections of the perfect tetrahedral network in the density range between 1.0 and 0.85 g/cm^3 arise from the presence of molecules with more than four neighbors—and not from the small fraction of three-coordinated molecules.

Table I shows also that for densities lower than 0.85 g/cm^3 there is a rapid increase in the number of three-coordinated molecules, while Fig. 2 shows that the average coordination number has become less than four. Also at ρ below 0.85, large cavities appear inside the liquid.[24] The appearance of three-coordinated molecules and of large cavities are related. In fact, close to the large cavities found in the low density simulations, one may expect behavior characteristic of the interface between water and flat hydrophobic surfaces[25] (molecules with an unbonded or dangling proton pointing toward the cavity). The small cavities that characterize the liquid for densities larger than 0.85 g/cm^3 can be created in the liquid without destroying the tetrahedral bonding network when the molecules adopt a straddling
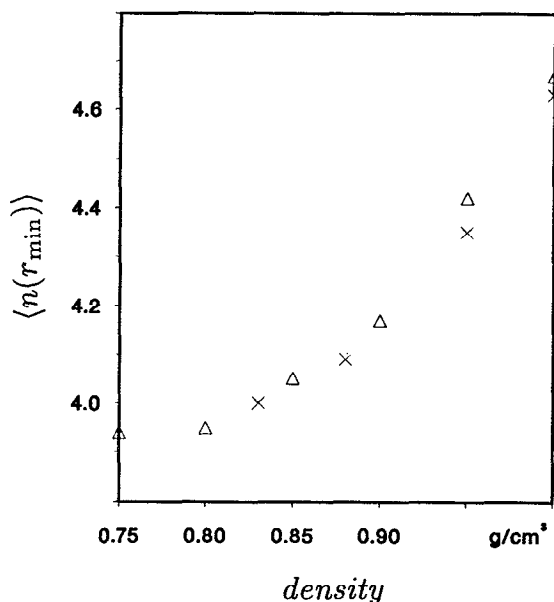
FIG. 2. Density dependence in ST2 water at 273 K (triangles) and 235 K (crosses) for the number of neighbors inside a shell of 3.3 Å. Here the number of neighbors is calculate using quenched configurations.
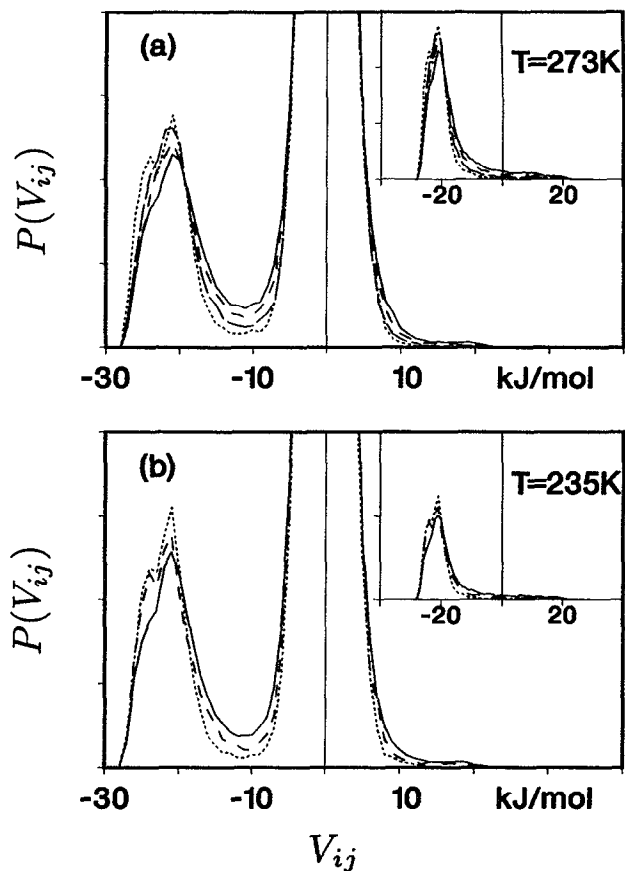

FIG. 3. Distribution function for the pair interaction energy V_{ij} for various densities, using the quenched configurations, as the density is decreased stepwise from $\rho = 1.0$ g/cm³. (a): Temperature $T = 273$ K, $\rho = 1$ (solid curve), 0.95 (short dashed curve), 0.9 (long dashed), 0.85 (dotted) g/cm³. (b): Temperature $T = 235$ K, $\rho = 1$ (solid), 0.95 (short dashed curve), 0.88 (dotted). The insets show the same $P(V_{ij})$ for all the pairs of molecules whose OO distance is less than 3.3 Å.

orientation with respect to the cavities—as found, for example, in clathrate structures or in the hydrophobic hydration shell.[16,26]

ENERGY DISTRIBUTION FUNCTIONS

More insight on the effect of decreasing the density can be obtained from the *pair energy* distribution function $P(V_{ij})$,[2] which is calculated from the quenched configurations and contains all the possible pair interaction energies V_{ij}. This function is plotted in Fig. 3 for $T = 235$ K and $T = 273$ K. The peak centered at $V_{ij} = 0$ is due mainly to the dipolar interactions between distant molecules, while the peak centered about -20 kJ/mol is due to the hydrogen bonding interactions. The insets show $P(V_{ij})$ for the pairs of molecules whose OO distance is less than 3.3 Å (the first neighbor shell). Figure 3 shows clearly that decreasing the density leads to a strong decrease of the amplitude of $P(V_{ij})$ for energies in the range above -18 kJ/mol and to a small increase of $P(V_{ij})$ for energies around -22 kJ/mol. Note that the insets of Fig. 3 confirm that the principal differences observed in Fig. 3 arise from changes in the first neighbor shell.

The presence of the extra molecule in the first coordination shell reduces the tetrahedrality of the force field produced by the molecular interactions and introduces new local minima in the potential energy hypersurface. To support this statement, consider the total binding energy distribution function $P(E_i)$ for the total binding energy $E_i \equiv \Sigma_j V_{ij}$; the sum extends over $j \neq i$ and $r_{ij} < r_c = 7.8$ Å. $P(E_i)$ is plotted in Fig. 4 for several values of density (using the quenched configurations). Note that $P(E_i)$ is broad and asymmetric for $\rho = 1$, and becomes much narrower and less asymmetric as ρ decreases. Note also that the position of the peak does

not shift with density. Lowering the density decreases the number of molecules whose energies lie (i) in the low energy tail (below -125 kJ/mol) and (ii) in the high energy tail ($E > -100$ kJ/mol).

We can interpret both decreases in terms of a reduction in the number of defects in the tetrahedral network. Accordingly, in Fig. 5 we show as a function of total binding energy the average coordination number $\langle n(r_{min}) \rangle_{E_i}$—i.e., the number of neighbors inside a shell of 3.3 Å averaged over all the molecules with the same binding energy. We observe that $\langle n(r_{min}) \rangle_{E_i}$ is enhanced for energies below, as well as above, the "perfect tetrahedral network" peak in $P(E_i)$ at about -115 kJ/mol. The existence of the low-energy tail shows that an extra molecule can fit in the the first coordination shell in such a way as to actually *increase* the magnitude of the total bonding energy. This can be understood if there exists a "bonded state" with more than four strong interactions—i.e., if there exist bifurcated bonds. Quantum mechanical calculations on clusters of water molecules have shown that a symmetric energy-optimized bifurcated HB is somewhat stronger than a conventional linear bond
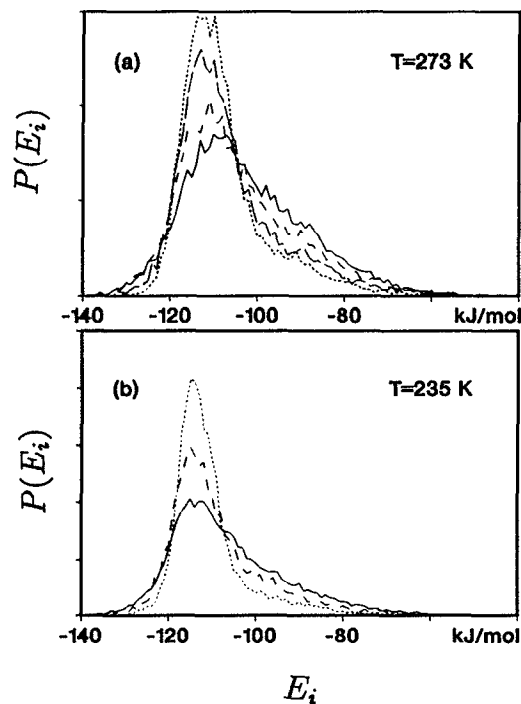
FIG. 4. Distribution function for the binding energy $E_i \equiv \Sigma_j V_j$ for various densities, using the quenched configurations. (a): Temperature $T = 273$ K, $\rho = 1$ (solid), 0.95 (short dashed curve), 0.9 (long dashed), 0.85 (dotted) g/cm³. (b): Temperature $T = 235$ K, $\rho = 1$ (solid), 0.95 (short dashed), 0.88 (dotted).

$(\delta E = -4$ kJ/mol).[27] Similar results have also been obtained for asymmetric bifurcated bonds.[28]

We also note that the effect of an extra molecule on $P(E_i)$ can be studied by decomposing $P(E_i)$ into the sum of Gaussian distribution functions. If we assume that each bond can be either bifurcated with probability p (if there is an extra molecule) or linear with probability $1 - p$, then
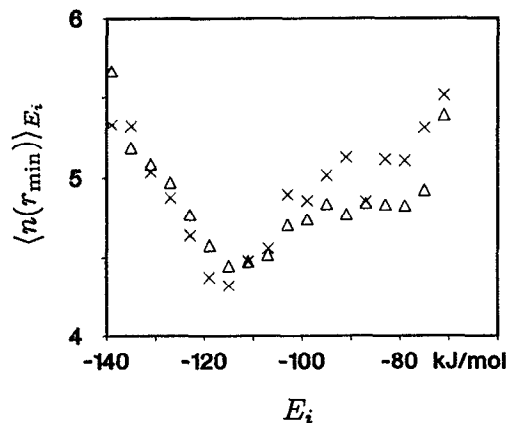

FIG. 5. $\langle n(r_{\min}) \rangle_{E_i}$, the number of neighbors inside a shell of 3.3 Å averaged over all the molecules with the same E_i as a function of the binding energy E, at 273 K (triangles) and 235 K (crosses) both for density 1.0 g/cm³. Note the enhancement for energies below—as well as above—the central perfect tetrahedral network peak in $P(E_i)$ at about -115 kJ/M. The total potential energy of the system is, with our definition, $(1/2)\Sigma_i E_i$ since each interaction V_{ij} is counted twice.

TABLE II. Results of the best fitting procedure for Eq. (1). Symbols are defined in the text.

	p	E_4	δE_{extra}	σ_4^2	$(\delta\sigma_{\text{extra}})^2$
			$T = 273$ K		
$\rho = 1.00$	0.24	-112	9.9	13.7	7.1
$\rho = 0.95$	0.19	-112	10.1	12.5	8.0
$\rho = 0.90$	0.135	-112	10.1	10.6	8.1
$\rho = 0.85$	0.096	-112	10.1	9.8	7.4
$\rho = 0.80$	0.086	-112	10.1	8.0	8.6
			$T = 235$ K		
$\rho = 1.00$	0.19	-114	10.4	12.0	7.2
$\rho = 0.95$	0.12	-114	10.6	9.6	6.4
$\rho = 0.88$	0.07	-114	10.5	7.6	5.9
$\rho = 0.83$	0.04	-114	10.5	7.8	0.5

$$P(E_i) \approx \sum_{l=0}^{4} \binom{l}{4} p^l (1-p)^{4-l} G_l. \tag{1}$$

Here G_l is a normalized Gaussian centered at an energy $E_l = E_4 + l(\delta E_{\text{extra}})$ with a width $\sigma_l^2 = \sigma_4^2 + l(\delta\sigma_{\text{extra}}^2)$. E_4 and σ_4 are the average energy and the variance for an environment with four neighbors, and δE_{extra} and $\delta\sigma_{\text{extra}}$ are the changes in average binding energy and variance associated with the extra molecule.

Table II shows the fitting parameters for different densities. Note that the probability of defect formation decreases by a factor of 3 on lowering the density. Note also that E_4, δE_{extra}, and the width of the Gaussian corresponding to extra molecules are roughly independent of density, while the width σ_4 of the Gaussian corresponding to a tetrahedral environment decreases when the density is lowered.[29] The quality of the fit for the lowest densities in Table II is less good since the fraction of three-coordinated molecules becomes significant at low densities (cf. Table I).

Figure 6 shows the decomposition of $P(E_i)$ using Eq. (1) for two different densities, 1.0 and 0.9 g/cm³. Also shown are the Gaussian components of this fit. Since the value of p is small, only three Gaussian components make a significant contribution to $P(E_i)$. We notice that the wings of the $P(E_i)$ distribution arise mainly from five or more coordinated molecules, a result consistent with our interpretation of the data shown in Figs. 4 and 5.

It is noteworthy that an analogous decomposition of the total binding energy in terms of different coordination numbers has been recently presented for amorphous silicon.[30] Also for this "almost tetrahedral" network (78% of the Si are four coordinated), the main imperfection arises from the presence of five-coordinated atoms (21%), and three coordinated atoms (1%). The defect-formation energy (the analog of our $\delta E_{\text{extra}}/2$) has been found to be 29 kJ/mol.[30,31] Interestingly, the ratio between the defect formation energy in silicon and water (29/5) is the same as the ratio of melting point temperatures (1665/273). Note that the change in structure on melting the two systems is similar; as seen from Table I, both systems pass from a perfect tetrahedral network to a mixture of four, five, and six coordinated units (also, note the similar values of the entropies of melting
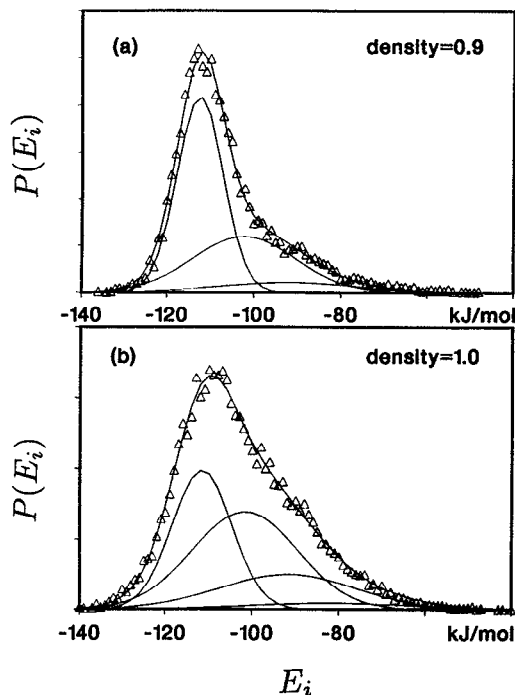
FIG. 6. Results of fitting the binding energy distribution function $P(E_i)$ (calculated from the quenched configurations) as in Eq. (1) for density (a) 1.0 g/cm³ and (b) 0.9 g/cm³, at temperature $T = 273$ K. Also shown are the Gaussian components as per Eq. (1).

FIG. 7. Distribution function for the binding energy E_i for densities $\rho = 0.8$ g/cm³ (full line) and $\rho = 0.75$ g/cm³ (dotted line) at $T = 273$ K, using the quenched configurations. The inset shows $\langle n(r_{\min}) \rangle_{E_i}$, the number of neighbours inside a shell of 3.3 Å averaged over all the molecules with the same E_i as a function of the binding energy E_i for the two densities. Note the region around -90 kJ/mol is populated by three coordinated molecules.

of water and Si). Hence the coincidence of the defect-energy and melting temperature ratios supports our fitting of $P(E_i)$ and also stresses the similar physics underlying the behavior of these two almost-tetrahedral networks.

At sufficiently low densities, the tetrahedral network begins to fragment, as seen in the very low density structural data presented in the previous section. Indeed, we find a new feature in the binding energy distribution, for $\rho < 0.85$. A clear peak emerges in $P(E_i)$ at an energy of about 20 kJ/mol above the strong peak corresponding to the four bonded molecules, as seen in Fig. 7 for densities 0.8 and 0.75 g/cm³. The inset shows $\langle n(r_{\min}) \rangle_{E_i}$ as a function of E_i for $\rho = 0.8$ (crosses) and 0.75 g/cm³ (triangles) and confirms the predominant contribution of three-coordinated molecules in the range around -90 kJ/mol.

MOLECULAR MOBILITY

The preceding two sections have provided evidence that lowering the density from 1.0 to 0.85 g/cm³ leads to a progressive decrease in the number of five-coordinated molecules and a slight increase in the number of three-coordinated molecules. If the mobility of the liquid were related to the local density (local free volume), then one would expect an increase in the molecular mobility on decreasing the density (as in normal liquids). Instead, the opposite trend is observed. In Fig. 8 we show the density dependence of the self-diffusion coefficient D, as calculated from the mean square displacement. Lowering the density by 10% decreases the

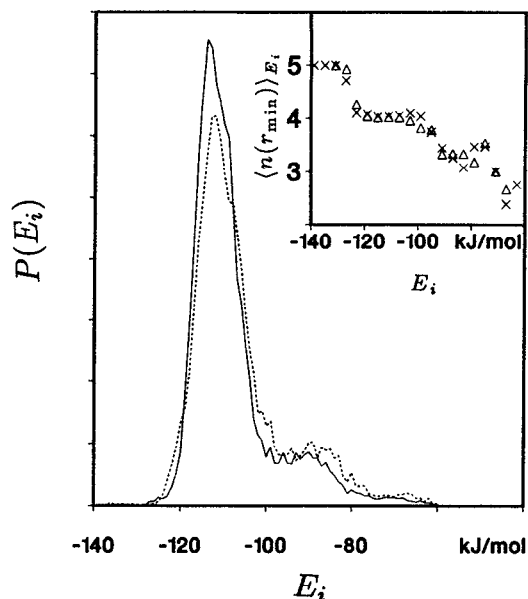diffusivity by a factor of 2 at 273 K and by a factor of 10 at 235 K. We find a similar sensitivity to density for the reorientational times.

Our results for the dependence of the mobility on the density support the hypothesis that the switching from one regular HB arrangement to another is facilitated by the local arrangement associated with the higher local density. To show that molecular mobility is enhanced in the presence of an extra molecule in the first coordination shell, we calculate the mean square displacement $\langle r^2(t) \rangle_n$ for groups of mole-
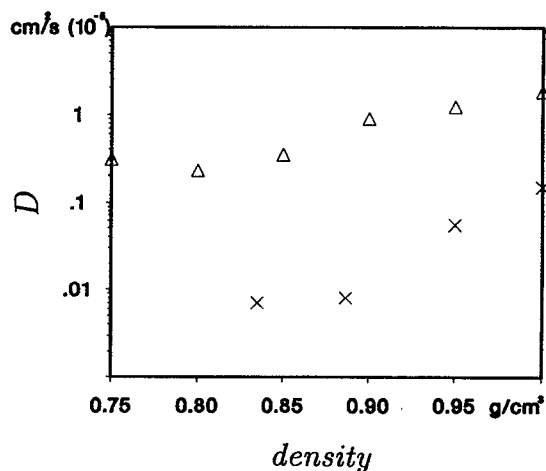

FIG. 8. Density dependence in ST2 water at 273 K (triangles) and 235 K (crosses) for the diffusion coefficient.

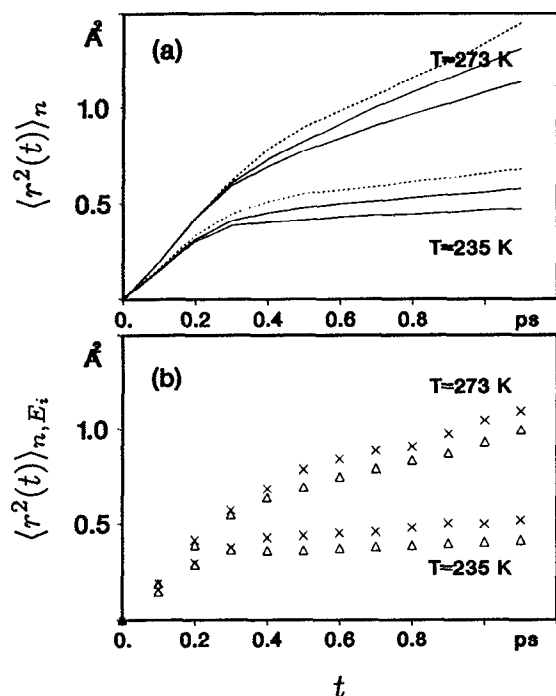FIG. 9. (a) Mean square displacement $\langle r^2(t)\rangle_n$ for groups of molecules with number of neighbors n equal to four (full line), five (dashed line), and six (dotted) for $T = 235$ and 273 K. (b) Mean square displacement $\langle r^2(t)\rangle_{n,E_i}$ for molecules with four (triangles) and five (crosses) neighbors and binding energy E_i between 110 and 115 kJ/mol.
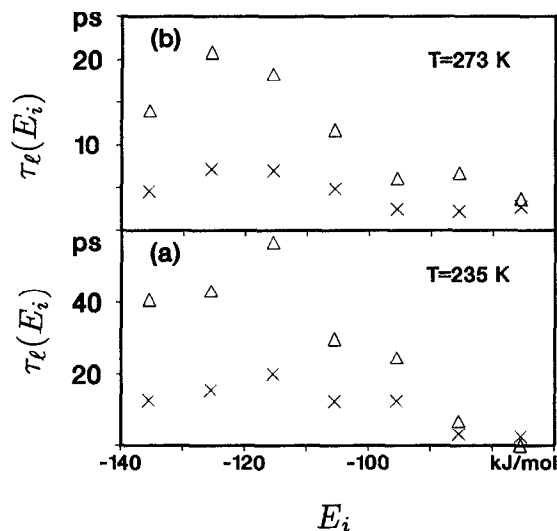

FIG. 10. Reorientational correlation times τ_1 (triangles) and τ_2 (crosses) as a function of the binding energy (calculated from the quenched configurations). (a) $T = 273$ K. (b) $T = 235$ K.

cules with number of neighbors n equal to four, five, and six. Fig. 9(a) shows $\langle r^2(t)\rangle_n$ calculated by following the time development of molecules for a time interval of 1.2 ps centered on a selected quenched configuration. The classification of the molecules according to the number of neighbors n is performed on the quenched configuration at the time $t = 0.6$ ps. We indeed find a significantly higher mobility for molecules with more than four neighbors.

To show that the higher mobility of the five-coordinated molecules is not only an effect of the average weaker bonding of these molecules, we show in Fig. 9(b) $\langle r^2(t)\rangle_{n,E_i}$ for molecules with the same E_i but different n. For both temperatures studied, the five-coordinated molecules move faster, suggesting that the energy barrier for translational diffusion is indeed lowered by the presence of an extra molecule in the first coordination shell.

Analogous results are obtained for rotational diffusion. In Fig. 10 we plot the reorientation times τ_1 (E_i) and τ_2 (E_i) as functions of E_i. These were calculated by following in the real simulation the time development of molecules whose binding energy from the quenched configuration is E_i, and by calculating the Legendre polynomial of order l, $\mathscr{P}_l = \langle \mathscr{P}_l [\cos(\theta)] \rangle$. $\theta = \theta(\tau)$ is the reorientational angle of the dipole direction. The P_l data between 0.6 and 1.2 ps have been fit to an exponential decay to extract the $\tau_l(E_i)$ values. The angular brackets denote an average over all molecules with binding energy E_i in the quenched configuration at the time $t = 0.6$ ps.

Comparing Fig. 10 and Fig. 5, we see a close correlation between local density and molecular reorientational times: Regions with higher local density are characterized by a faster dynamics. It is important to observe that five-coordinated molecules with very strong binding energies reorient themselves faster than the mainly four-bonded molecules contributing at — 115 kJ/mol. Thus the lowering of the energy barriers for the rotational motion (produced by the presence of an extra molecule) is not associated with a worse local bonding, but is instead related to the progressive reduction of the tetrahedrality of the interaction energy surface.[32] This supports the possibility that the bifurcated bonds—produced by the approach of a fifth molecule—may offer a path connecting different tetrahedral arrangements through activation barriers lower than the activation energy needed to break a linear HB.

Another confirmation that the presence of a fifth molecule indeed "catalyzes the reorganization of the local network," is found when we compare the shell occupation time correlation functions[7] for the four and five bonded molecules. This function gives information on how long a molecule which at time $t = 0$ belongs to the first neighbor shell remains in the vicinity of the same molecule. We find evidence for preferential exchange of molecules near the five or more bonded molecules, suggesting a higher mobility and a more rapid reshuffling of the network. In this respect, the conversion between coordination numbers of five and four can be one of the mechanisms on which the reorganization of the network is based.

Finally, we observe that the molecular mobility in other tetrahedrally connected networks (e.g., SiO_2 and BeF_2)[33,34] has been shown to be controlled by the number of five-coordinated defects. The elementary diffusive step in these glass-forming systems is related to the passage of an extra atom, and to the associated shift of the defect along the network. The different binding energies characterizing the

four and five coordination environment, together with this defect-propagation model, furnishes also a microscopic interpretation for the negative correlation between the changes of the binding energy of neighbor water molecules ("flip–flop mechanism") observed by Ohmine et al.[35]

DISCUSSION AND SUMMARY

In this paper we have used the dependence on the density of the dynamics in liquid water as a tool to clarify the relation between mobility and structure. We have presented data related to the stretched state of the liquid—the range of densities that are very recently becoming accessible to experimental study.[22]

We have found that in contrast to the behavior of normal liquids, lowering the density is associated with an increase in the structure of the liquid,[16] which is related to the decrease of the number of five or more coordinated molecules. Above $\approx 0.85 \cdot g/cm^3$ a global density decrease is achieved by reducing the number of nearest neighbors and increasing the overall tetrahedrality of the network. Below $0.8 \ g/cm^3$, further structural changes occur—an increase in the number of three-coordinated molecules, and the formation of large cavities.

By studying the binding energy we have shown that the extra molecules can fit in the first shell in a wide variety of modes. Interestingly, there exist local arrangements with five neighbors with total energy lower than the perfect tetrahedral arrangement. This is rationalized in terms of bifurcated interactions, where one of the protons of the central molecule is pointing toward two neighbor oxygens or where three protons from three different neighbor atoms point toward the central oxygen.

We also found that the mobility in the system is associated with the presence of extra molecules in the first coordination shell. We demonstrated that molecules with five neighbors diffuse faster than four-coordinated molecules, even when the five-coordinated molecules are strongly bonded. Thus the presence of extra molecules offers a path connecting different network arrangements through activation barriers lower than the activation energy needed to break a linear HB. Thus the presence of extra molecules in the first coordination shell serves as a catalyst for the restructuring of the hydrogen bond network when the thermal energy kT is much smaller than the hydrogen bond energy.

Moreover, the decreased mobility—as well as the increased structural order in hydrophobic hydration shells[26,36]—can be understood as a consequence of the lower local density of water, due to the fact that the water is effectively "locally diluted" by the (inert) hydrophobic particle. The presence of the inert hydrophobic particle prevents the hydration shell water molecules from being approached by more than four other molecules, thus preventing the creation of low activation energy barriers and thus slowing down the molecular mobility.[37] The opposite effect—the creation of increased mobility by increasing the (global) density—is the experimentally well known "anomalous motional behavior" of water under compression.[38,39]

[1] For recent reviews with extensive literature references, see C. A. Angell, Annu. Rev. Phys. Chem. 34, 593 (1983); Hydrogen Bonded Liquids, edited by J. Dore and J. Teixeira (Kluwer, Dordrecht, 1991).

[2] F. H. Stillinger and A. Rahman, J. Chem. Phys. 60, 1545 (1974).

[3] O. Matsuoka, E. Clementi, and M. Yoshimine, J. Chem. Phys. 64, 1351 (1976); U. Niesar, G. Corongiu, E. Clementi, G. R. Kneller, and D. K. Bhattacharya, J. Phys. Chem. 84, 7949 (1990).

[4] H. J. C. Berendsen, J. P. M. Postma, W. F. von Gunsteren, and J. Hermans, in Intermolecular Forces, edited by B. Pullman (Reidel, Dordrecht, 1981), p. 331.

[5] W. L. Jorgensen, J. Chandrasekhar, J. D. Madura, R. W. Impey, and M. L. Klein, J. Chem. Phys. 79, 926 (1983).

[6] M. Mezei and D. L. Beveridge, J. Chem. Phys. 74, 622 (1981); R. J. Speedy, J. D. Madura, and W. L. Jorgensen, J. Phys. Chem. 91, 909 (1987).

[7] D. A. Zichi and P. J. Rossky, J. Chem. Phys. 84, 2814 (1986).

[8] A. Geiger, F. H. Stillinger, and A. Rahman, J. Chem. Phys. 70, 4185 (1979).

[9] H. E. Stanley and J. Teixeira, J. Chem. Phys. 73, 3404–3422 (1980); H. E. Stanley, J. Teixeira, A. Geiger, and R. L. Blumberg, Physica A 106, 260 (1981); R. L. Blumberg, H. E. Stanley, A. Geiger, and P. Mausbach, J. Chem. Phys. 80, 5230 (1984).

[10] F. Sciortino, P. H. Poole, H. E. Stanley, and S. Havlin, Phys. Rev. Lett. 64, 1686 (1990).

[11] See, for example, the discussion in E. Grünwald, J. Am. Chem. Soc. 108, 5719 (1986).

[12] A. H. Narten and H. A. Levy, Science 165, 447 (1969).

[13] P. A. Giguère, J. Chem. Phys. 87, 4835 (1987). See also Fig. 9 of G. E. Walrafen, M. S. Hokmabadi, W.-H. Yang, Y. Chu, and B. Monosmith, ibid. 93, 2909 (1989).

[14] R. Lippincott and R. Schroeder, J. Chem. Phys. 23, 1099 (1955); G. Walrafen, in Water: A Comprehensive Treatise, Vol. 1 edited by F. Franks (Plenum, New York, 1972), Chap. 5; G. E. Walrafen, M. S. Hokmabadi, and W. H. Yang, J. Phys. Chem. 92, 2433 (1988); G. E. Walrafen, ibid. 94, 2237 (1990); S. Krishnamurthy, R. Bansil, and J. Wiafe-Akenten, J. Chem. Phys. 79, 5863 (1983); G. E. Walrafen, M. R. Fisher, M. S. Hokmabadi, and W.-H. Yang, ibid. 85, 6970 (1986).

[15] F. X. Prielmeier, E. W. Lang, H. D. Lüdemann, and R. J. Speedy, Phys. Rev. Lett. 59, 1128 (1987).

[16] A. Geiger, P. Mausbach, and J. Schnitker, in Water and Aqueous Solutions, edited by G. W. Neilson and J. E. Enderby (Adam Hilger, Bristol, 1986).

[17] M. H. Cohen and D. Turnbull, D. J. Chem. Phys. 31, 1164 (1959).

[18] F. Sciortino, A. Geiger, and H. E. Stanley, Phys. Rev. Lett. 65, 3452 (1990).

[19] On the possibility that bifurcated bonds are connected to mobility, see also Y. Naberukhin, J. Struct. Chem. 25, 223 (1984).

[20] F. H. Stillinger and T. A. Weber, J. Phys. Chem. 87, 2833 (1983).

[21] Removing bonding ambiguities through quenching processes is discussed in T. A. Weber and F. H. Stillinger, J. Chem. Phys. 87, 3252 (1987).

[22] C. A. Angell, Nature (London) 331, 206 (1988); J. L. Green, D. J. Durben, G. H. Wolf, and C. A. Angell, Science 249, 649 (1990).

[23] It is interesting to note that the density of 0.80–0.85 g/cm³ is in agreement with the density extrapolated by R. Speedy [J. Phys. Chem. 86, 982 (1982)] for the conjectured spinodal line which limits the region of metastability.

[24] A. Geiger and P. Mausbach, in Hydrogen Bonded Liquids, edited by J. Dore and J. Teixeira (Kluwer, Dordrecht, 1990); see also N. N. Medvedev and A. Geiger (to be published).

[25] C. Y. Lee, J. A. McCammon, and P. J. Rossky, J. Chem. Phys. 80, 4448 (1984).

[26] A. Geiger, A. Rahman, and F. H. Stillinger, J. Chem. Phys. 70, 273 (1979).

[27] M. D. Newton, J. Phys. Chem. **87**, 4288 (1983).

[28] M. D. Newton, G. A. Jeffrey, and S. Takagi, J. Am. Chem. Soc. **101**, 1997 (1979).

[29] The average weakening of the binding energy by 10 kJ/mol (cf. the column of Table II labeled δE_{extra}) associated with an extra molecule compares well with the energy difference chosen to interpret the temperature dependence of dynamic as well as thermodynamic quantities in liquid water with two-state models (Ref. 11).

[30] W. D. Luedtke and U. Landman, Phys. Rev. B **40**, 1164 (1989).

[31] S. T. Pantelides, Phys. Rev. Lett. **57**, 2979 (1986).

[32] It is important to stress the differences of our finding with the model of Robinson and co-workers [G. W. Robinson, J. Lee, K. G. Casey, and D. Statman, Chem. Phys. Lett. **123**, 483 (1986); M. P. Bassez, J. Lee, and G. W. Robinson, J. Phys. Chem. **91**, 5818 (1987)]. We explain the progressive sphericalization of the neighbor field by the presence of an extra molecule and the faster dynamics with the creation of new local minima separated by lower activation energies. Robinson and co-workers assume instead that the thermal activated rotations produce a sphericalized average field and an associated lowering of the activation energies of the neighboring molecules. But to fit the temperature dependence of the density they assume a higher local density around the rotating molecules.

[33] L. V. Woodcock, C. A. Angell, and P. Cheeseman, J. Chem. Phys. **64**, 1566 (1976); C. A. Angell, Mater. Res. Soc. Symp. **63**, 85 (1985).

[34] S. A. Brawer, J. Chem. Phys. **75**, 3516 (1981).

[35] H. Tanaka and I. Ohmine, J. Chem. Phys. **87**, 6128 (1987); I. Ohmine, H. Tanaka, and P. G. Wolynes, *ibid.* **89**, 5852 (1988); H. Tanaka and I. Ohmine, *ibid.* **91**, 6318 (1989).

[36] J.-Y. Huot and C. Jolicoeur, in *The Chemical Physics of Solvation*, edited by R. R. Dogonadze, E. Kalman, A. A. Kornyshew, and J. Ulstrup (Elsevier, Amsterdam, 1985).

[37] Recently, U. Kaatze and R. Pottel (preprint) demonstrated a universal speeding up of dielectric relaxation with increasing spatial density of H-bond forming molecules in various mixtures of water with predominantly hydrophobic particles.

[38] E. W. Lang and H. D. Lüdemann, in *High Pressure NMR*, edited by J. Jonas (Springer, Berlin, 1991).

[39] R. Pottel, E. Asselborn, R. Eck, and V. Tresp, Ber. Bunsenges. Phys. Chem. **93**, 676 (1989).